TIMING AND HISTORY OF METAMORPHISM IN THE CENTRAL GNEISS COMPLEX

ERIC BUTLER
Department of Geology, Beloit College
Faculty Sponsor: Cam Davidson, Beloit College

INTRODUCTION

The Central Gneiss Complex (CGC) is a unit of high-grade, partially migmaticic ortho- and paragneisses intruded by diorite and tonalite plutons located in the coastal mountains of British Columbia. The CGC is contained within the Coast Plutonic Complex (CPC), a magmatic arc extending over 800 km from Alaska to Washington that marks the contact between the Insular and Intermontane Superterranes (Monger et al., 1982; Davidson et al., this volume).

Several studies have defined P-T paths for the CGC. Selverstone and Hollister (1980) calculated the peak metamorphic conditions to be 4.2-5.5 Kb and 725-775°C. Crawford and Hollister (1982) described andalusite-bearing veins cross-cutting the gneissic fabric, providing a low-pressure terminus for the P-T path. The generally accepted P-T model for the CGC involves an early high-pressure phase, recorded by staurolite + garnet + kyanite, followed by heating that moved the rocks into the sillimanite stability field. Hollister (1982) proposed that the CGC was then uplifted rapidly (2 mm/yr) from approximately 35 km depth to around 5 km between 64 and 48 Ma.

The purpose of this study is to define the P-T-t path of the CGC by presenting new geothermobarometric data calculated from mineral assemblages and reaction textures. In addition, the U+ and Th content of monazite is measured in high-grade sillimanite gneisses to test the viability of constraining the timing of metamorphism in the CGC.

GEOLOGIC SETTING

The rocks of the CGC are mostly amphibolite to granulite facies gneisses, with minor calc-silicate and amphibolite layers. Foliations in the CGC generally strike north-northwest and dip steeply to moderately east-northeast, parallel with lithologic layering. Folds range in size from centimeter to kilometer scale, mostly tight to isoclinal with steeply east-dipping axial surfaces and shallow to moderately north-plunging hinges (Andronicus et al., 1999). The gneisses can be divided into two distinct units that are recognizable in the field by their differing weathering characteristics; those that weather grey, and those that weather rusty brown. The differences in weathering reflect differences in composition and protolith. The grey gneisses are composed of quartz + plagioclase + biotite ± hornblende and are interpreted by Crawford et al. (1987) to be metamorphosed andesitic lava flows or tonalite sills. The rusty gneisses are composed of quartz + plagioclase + biotite ± sillimanite ± garnet and are interpreted to be metasedimentary in origin. Within the rusty gneisses are units of extremely aluminous gneiss that contain 30% - 60% coarse-grained sillimanite and garnet (Hollister and Andronicus, 2000).

The aluminous rusty gneisses contain several useful mineral assemblages and reaction textures. Hollister (1982) described both kyanite and staurolite preserved in garnets, as well as the assemblage sillimanite + staurolite + hercynite. Sillimanite pseudomorphs of kyanite are widespread in the matrix (Crawford and Hollister, 1987), some over 1 cm in length. In addition, Hollister (1982) described several low-pressure mineral assemblages apparently replacing higher-temperature ones. These include garnet + sillimanite + quartz = cordierite and garnet + biotite + sillimanite = cordierite + hercynite + orthoclase.

REACTION TEXTURES AND GEOTHERMOBAROMETRY

Samples of the rusty weathering paragneiss were collected from the southern CGC (see Fig. 2., Davidson et al., this volume) to look for reaction textures and metamorphic monazite. Typical mineral assemblages consist of quartz + plagioclase + biotite with 0-20% grt and 0-10% sillimanite. Some layers are extremely aluminous, containing up to 30% sillimanite and 25% garnet.

The matrix of most samples consists of quartz and plagioclase, with the foliation defined by biotite and sillimanite. Sillimanite ranges in size from fibrolite to large, blocky crystals 2 mm or more in length. In the field, coarse sillimanite occurs as > 1 cm pseudomorphs after kyanite (Fig. 1a).

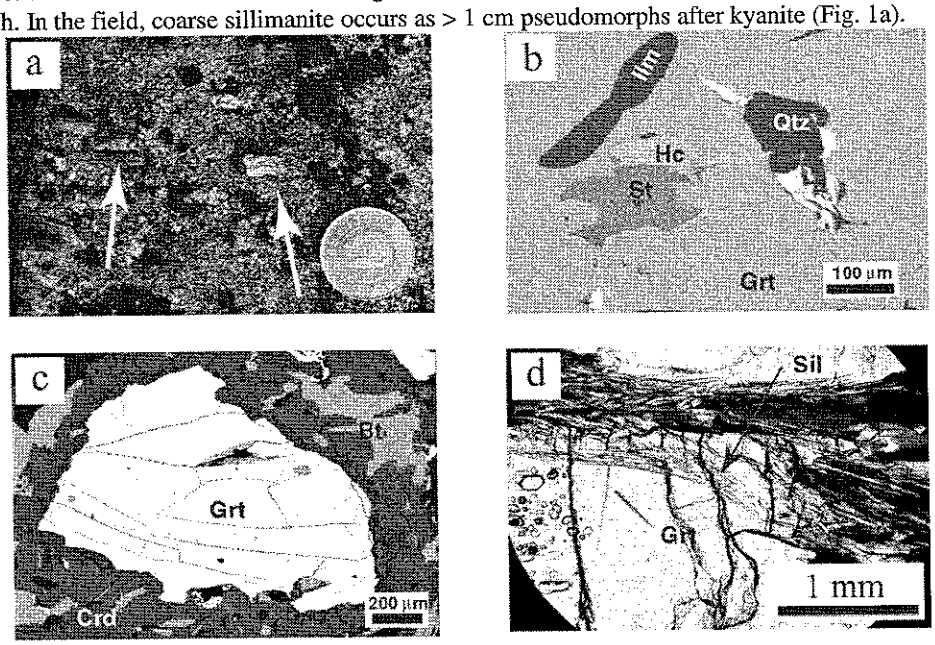

Figure 1. Reaction textures from the Central Gneiss Complex. (a) Sillimanite after kyanite pseudomorphs: coin is 2 cm across (b) Mg X-ray map of staurolite and hercynite inclusions in garnet: brighter areas indicate higher concentrations of magnesium. (c) BSE image of cordierite rims on garnet. (d) Garnet overgrowth of sillimanite + biotite fabric.

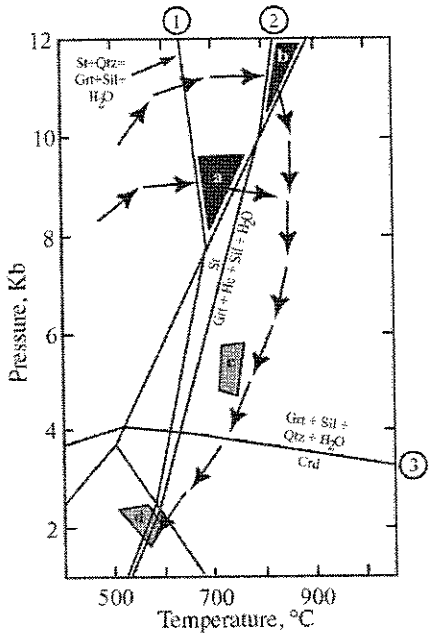

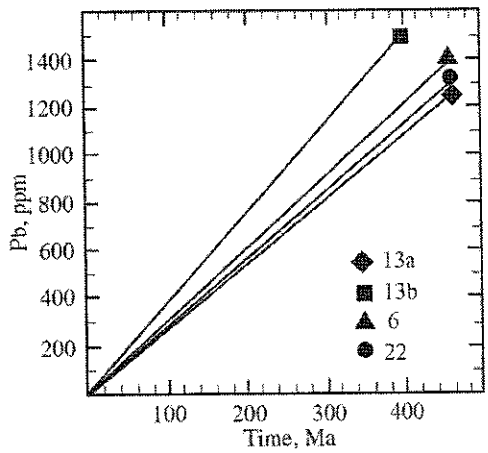

Figure 3. Accumulation of radiogenic Pb in monazite over time. Calculated from U-Th elemental concentrations using the age equation from Montel et al. (1996). Number labels refer to individual crystals.

Figure 2. Proposed P-T paths for the Central Gneiss Complex. Black polygons represent possible early high-pressure events (a) minimum peak pressure (b) potential peak pressure. Grey polygons represent P-T conditions described by(c) Selverstone and Hollister (1980) and (d) Crawford and Hollister (1982). See text for discussion. Reactions (1) and (2) calculated using TWQ (Berman et al., 1991) using Fe end members. Reaction (3) calculated using mineral data from 96 PR-71. Abbreviation used: St (staurolite), Qtz (quartz), Grt (garnet), Sil (sillimanite), Crd (cordierite).

Garnet occurs as porphyroblasts 1-5 mm in diameter and typically contains inclusions of quartz and plagioclase with minor biotite, ilmenite, zircon, and monazite. Garnet in the sillimanite-rich gneisses also contains inclusions of kyanite and staurolite reacting to form hercynite (Fig. 1b). When present, cordierite forms thick reaction rims around garnet (Fig. 1c). Many garnets contain sillimanite-rich rims that appear to overgrow over the foliation defined by sillimanite and biotite (Fig. 1d).

Figure 2 shows two possible P-T paths for the southern CGC. Reactions (1) and (2) were calculated using TWQ (Berman, 1991) using Fe endmembers (Berman, 1988, 1990). Using Fe end-members provides a minimum temperature constraint because the addition of Mg moves the curve towards higher temperatures. Reaction (3) was calculated using mineral data from 96 PR-71. The shaded regions show calculated or inferred P-T conditions.

U-Th-Pb DATING OF MONAZITE

A number of recent studies have successfully used the U-Th-Pb contents of monazite measured on the electron microprobe to date crystal growth (Suzuki et al., 1994; Montel et al., 1996; Braun et al., 1998; Williams et al., 1999). Monazite, a rare-earth phosphate, contains many rare-earth elements including U, Th, Ce, La, and Nd. Monazite grows during metamorphism and is most commonly found in pelitic schists and gneisses of upper amphibolite to granulite faces (Parrish, 1990).

The closure temperature of monazite appears to be high (725 - 750°C), so it is an ideal candidate for dating high-T metamorphic events (Copeland et al., 1998; Parrish, 1990, Braun et al., 1998). Monazite incorporates significant amounts of U and Th upon crystallization, allowing radiogenic Pb to build up quickly. In addition, because common (non-radiogenic) lead is excluded from the monazite crystal during crystallization, all the lead measured in a monazite crystal is from the decay of U + Th since crystallization (Parrish, 1990). This allows a date to be calculated from the elemental abundances of U, Th, and Pb (Montel et al., 1996).

For this study we used the University of Wisconsin-Madison's Cameca SX-50 electron microprobe to see if the Pb content of monazite from a garnet-sillimanite gneiss (EB-50-2) from the CGC was above the 1,000 ppm detection limit. To achieve a 1000 ppm detection limit, we counted for 120s with a 20 kV acceleration voltage and 150 nA beam current. Lower detection limits could be achieved with longer count times and/or higher beam currents: Montel et al. (1996) reported achieving a 200 ppm detection limit. Pb levels in the four monazite crystals we measured were below 1000 ppm; however, we were able to measure the U and Th concentrations (Table 1). Even without detectable Pb, the measured U and Th concentrations constrain the age of the monazites to be less than 275-375 Ma (Fig. 3).

TABLE 1. Electron microprobe analysis of monazite

	Oxide percents											ppm	
crystal #	U_3O_8	ThO_2	Ce_2O_3	Nd_2O_3	La_2O_3	Y_2O_3	P_2O_5	CaO	SiO_2	Sm_2O_3	Oxide Totals	U	Th
13a	0.447	5.514	26.932	18.748	10.114	1.266	31.038	0.535	0.512	3.924	99.030	3790	48458
13b	0.201	8.954	25.287	18.902	9.130	1.104	30.744	0.601	0.713	3.504	99.140	1707	78687
6	1.562	2.883	25.175	14.477	10.266	2.991	32.935	0.658	1.420	3.673	96.040	13249	25343
22	0.798	4.696	26.804	17.591	9.222	2.337	32.676	0.843	0.178	2.847	97.992	6769	41266

DISCUSSION

Abundant sillimanite pseudomorphs of kyanite as well as staurolite and kyanite inclusions in garnet indicate an early high-pressure event in the CGC. The presence of staurolite reacting to hercynite raises the question of where in P-T space this reaction took place. If this occurred in the sillimanite field, the maximum pressure reached was around 8-9 Kb (a, Fig. 2). However, samples that contain kyanite and staurolite/hercynite inclusions in garnet, raise the possibility that this reaction took place in the kyanite stability field. This would indicate a higher peak pressure, around 11-12 Kb (b, Fig. 2). Thick cordierite reaction rims on garnet support Hollister's (1982) description of rapid uplift. In this scenario, the rocks pass through the P-T conditions calculated by Selverstone and Hollister (1980) (c, Fig. 2) during the rapid decompression phase and reach the andalusite-stable field at the location described by Crawford and Hollister (1982) (d, Fig. 2).

The results of the U-Th-Pb dating of monazite attempted in this study indicate that crystals 50 to 100 Ma from the CGC can be dated using the electron microprobe with detection limits between 200-300 ppm (Fig. 3). This suggests that U-TH-Pb dating of monazite in the CGC might be possible, especially in rocks that contain higher concentrations of U and Th.

CONCLUSIONS

Metamorphism of the CGC resulted in a clockwise P-T path, beginning with an early high-pressure event followed by heating into the sillimanite field and subsequent rapid uplift. This path is documented by kyanite and staurolite inclusions in garnet and cordierite reaction rims on garnet. These data confirm the previous P-T work by Selverstone and Hollister (1980), Hollister (1982), and Crawford et al. (1987). The presence of staurolite to hercynite reactions along with kyanite in garnet cores suggests that the CGC may have reached higher pressures than previously thought (11-12 kb). In addition, U-Th-Pb dating of monazite on the electron microprobe has the potential to constrain the timing of metamorphism in the CGC.

REFERENCES

Andronicus, C.L., Hollister, L.S., Davidson, C., and Chardon, D., 1999, Kinematics and tectonic significance of transpressive structures within the Coast Plutonic Complex, British Columbia: Journal of Structural Geology, v. 21, p. 229-243.

Berman, R.G., 1988, Internally-consistent thermodynamic data for stoichiometric minerals in the system Na2O-K2O-CaO-MgO-FeO-Fe2O3-Al2O3-SiO2-TiO2-H2O-CO2: Journal of Petrology, v. 29, p. 445-522.

Berman, R.G., 1990, Mixing properties of Ca-Mg-Fe-Mn garnets: The American Mineralogist, v. 75, p. 328-344.

Berman, R.G., 1991, Thermobarometry using multiequilibrium calculations: a new technique with petrologic applications: Canadian Mineralogist, v. 29, p. 833-855.

Braun, I., Montel, J., and Nicollet, C., 1998, Electron microprobe dating of monazites from high-grade gneisses and pegmatites of the Kerala Khondalite Belt, southern India: Chemical Geology, v. 146, p. 65-85.

Copeland, P., Parrish, R.R., and Harrison, T.M., 1988, Identification of inherited radiogenic Pb in monazite and its implications for U-Pb systematics: Nature, v. 333, p. 760-763.

Crawford, M.L., Crawford, W.A., and Gehrels, G.E., 1999, Terrane assembly and structural relationships in the eastern Prince Rupert quadrangle, British Columbia: Geological Society of America Special Paper, v. 343, p. 1-21.

Crawford, M.L., and Hollister, L.S., 1982, Contrast of metamorphic and structural histories across the Work Channel lineament, Coast Plutonic Complex, British Columbia: Journal of Geophysical Research, v. 87, p. 3849-3860.

Crawford, M.L., Hollister, L.S., and Woodsworth, G.J., 1987, Crustal deformation and regional metamorphism across a terrane boundary, Coast Plutonic Complex, British Columbia: Tectonics, v. 6, p. 343-361

Hollister, L.S., 1982, Metamorphic evidence for rapid (2 mm/yr) uplift of a portion of the Central Gneiss Complex, Coast Mountains, B.C.: Canadian Mineralogist, v. 20, p. 319-332.

Hollister, L.S., and Andronicus, C.L., 2000, The Central Gneiss Complex, Coast Mountains, British Columbia: Geological Society of America Special Paper, v. 343, p.45-59.

Monger, J.W.H., Price, R.A., and Tempelman-Kluit, D.J., 1982, Tectonic accretion and the origin of the two major metamorphic and plutonic welts in the Canadian Cordillera: Geology, v. 10, p. 70-75.

Montel, J., Foret, S., Veschambre, M., Nicollet, C., and Provost, A., 1996, Electron microprobe dating of monazite: Chemical Geology, v. 131, p. 37-53.

Parrish, R.R., 1990, U-Pb dating of monazite and its application to geological problems: Canadian Journal of Earth Science, v. 27, p. 1431-1450.

Selverstone, J., and Hollister, L.S., 1980, Cordierite-bearing granulites from the Coast Ranges, British Columbia: P-T conditions of metamorphism: Canadian Mineralogist, v. 18, p. 119-129.

Williams, M.L., Jercinovic, M.J., and Terry, M.P., 1999, Age mapping and dating of monazite on the